The Determination of Lateral Diffusivity in Diabatic Conditions near the Ground from Diffusion Experiments

GIICHI YAMAMOTO[1]

U. S. Weather Bureau, Washington, D. C.

AND ATSUSHI SHIMANUKI

Geophysical Institute, Tohoku University, Sendai, Japan

(Manuscript received 28 October 1963, in revised form 16 December 1963)

ABSTRACT

The three-dimensional equation of diffusion is solved numerically. Vertical diffusivity derived from the turbulent transfer theory is used, as is an assumed form for the lateral diffusivity containing an unknown parameter with respect to stability. The parameter is determined as a function of stability by comparing the theoretical distribution of concentration with observations made during projects Prairie Grass and Green Glow. The dependence on the averaging time of the lateral diffusivity of smoke concentration is also estimated by use of these experiments. The diffusion patterns in different stability and surface conditions are expressed fairly well by the calculations.

1. Introduction

Although the statistical theory of turbulence originated by G. I. Taylor has been seen to be useful in describing the diffusion process in a homogeneous turbulent flow, this approach seems to be very difficult for the study of diffusion in diabatic shear flow in the atmospheric surface layer. On the other hand, the recent developments of the turbulent transfer theory, for instance, by Monin and Obukhov (1954), Ellison (1957), Yamamoto (1959), and Panofsky, Blackadar and McVehil (1960) have shown that the diabatic wind profile could be derived fairly well from the turbulent transfer theory. This means that the vertical eddy diffusivity introduced in the theory is reasonable in diabatic conditions. From this point of view, the present authors (Yamamoto and Shimanuki, 1960) have investigated the two-dimensional problem (diffusion from a line source) in diabatic conditions by solving numerically the equation of diffusion in which the vertical diffusivity inferred from the transfer theory was used.

The next step of our research was to investigate the three-dimensional diffusion from a point source in a diabatic atmosphere, following the line of our previous research. However, a serious difference exists between the two-dimensional and the three-dimensional problems. While the vertical diffusivity could be inferred from the study of vertical profiles of wind velocity and temperature, the behavior of the lateral diffusivity is scarcely known at present. One of the clues to infer the nature of the lateral diffusivity is obviously the observed three-dimensional diffusion patterns themselves, although the effect of the lateral diffusivity is therein complicated. In this paper we report an evaluation of lateral diffusivity made by comparing the solution of the three-dimensional diffusion equation with observations. The solution of the equation which involves the evaluated lateral diffusivity gives us a detailed diffusion pattern.

[1] Now at Geophysical Institute, Tohoku University, Sendai, Japan.

2. Eddy diffusivities

According to the turbulent transfer theories cited above, if equality of diffusivities for momentum and heat is assumed, the vertical diffusivity K_z is given by

$$K_z = k^2 z^2 \frac{du}{dz}(1-\sigma R_i)^{\frac{1}{2}} = k z_0 u_* \xi / \varphi, \tag{1}$$

with

$$\varphi^4 + \zeta \varphi^3 - 1 = 0, \tag{2}$$

$$\varphi(\zeta) = \zeta \frac{df}{d\zeta}, \tag{3}$$

$$f = ku/u_*, \tag{4}$$

$$\xi = z/z_0 = \zeta/\zeta_0, \tag{5}$$

$$\zeta = -\sigma z/L, \tag{6}$$

$$\zeta_0 = -\sigma z_0/L, \tag{7}$$

and

$$L = -u_*^3 T_0 C_p \rho/(kgq). \tag{8}$$

k is von Karman's constant, equal to 0.41, σ a numerical factor of about 13 (Deacon, 1949, and Kondo, 1962) or 18 (Panofsky *et al.*, 1960), R_i the Richardson number, u_* the friction velocity, z_0 the roughness parameter, L the stability length introduced by Monin and Obukhov (1954), and ζ the non-dimensional stability parameter (Yamamoto, 1959). Other symbols are familiar and need not be noted here.

On the other hand the relation between lateral diffusivity and stability is not known, and it is one of the aims of the present study to establish this relation, at least empirically. For this purpose the lateral diffusivity was assumed to have a simple form involving an unknown parameter with respect to stability. The diffusion equation, which involves both the vertical diffusivity derived from the transfer theory and the assumed lateral diffusivity, was solved numerically. A part of the numerical solution was then compared with the observational data to determine the unknown parameter in the assumed expression. Next the other parts of the solution with the determined lateral diffusivity were compared with the data to test the validity of the assumption. A reasonable relation between the lateral diffusivity and stability was established by this method. The calculated results, being the solution of the diffusion equation, give us a detailed pattern on diffusion from a point source, which will be applicable as such for any meteorological and surface conditions.

In this study, after several trials, the lateral diffusivity K_y was assumed to be of the following form:

$$K_y/kz_0u_*=\alpha(\zeta_0)\xi. \tag{9}$$

α is an unknown function of ζ_0, which is to be determined numerically by comparison of the calculated and observed diffusion patterns. The assumed height dependence of K_y is a simple one, being the same as that of K_z in neutral conditions. Other parameters in (9), i.e., k, z_0 and u_*, are introduced in analogy to (1). It should be noted that the unknown function α in (9) will also depend on the averaging time T. The averaging time, which is defined by the time interval over which the concentration of smoke is to be averaged, is also equivalent to the time at which the smoke is released from the source, provided that the smoke is collected over a sufficiently long time interval. It is known that the horizontal dispersion of smoke increases with T. (See, for instance, Shimanuki, 1961.) In the present study we have examined the Prairie Grass data (Barad, 1958) with $T=10$ minutes and the Green Glow data (Barad and Fuquay, 1962) with $T=30$ minutes. The dependence of α on T will be found by use of these two groups of data.

3. The equation of diffusion and a procedure for solving it

The steady-state equation for diffusion from a continuous point source is given by

$$u\frac{\partial\chi}{\partial x}=\frac{\partial}{\partial y}\left(K_y\frac{\partial\chi}{\partial y}\right)+\frac{\partial}{\partial z}\left(K_z\frac{\partial\chi}{\partial z}\right), \tag{10}$$

where χ is the non-dimensional concentration of smoke. Substituting (1), (4) and (9) into (10), we obtain the following dimensionless diffusion equation:

$$\frac{f}{k^2}\frac{\partial\chi}{\partial(x/z_0)}=\frac{\partial}{\partial(y/\alpha^{\frac{1}{2}}z_0)}\left(\xi\frac{\partial\chi}{\partial(y/\alpha^{\frac{1}{2}}z_0)}\right)+\frac{\partial}{\partial\xi}\left(\frac{\xi}{\varphi}\frac{\partial\chi}{\partial\xi}\right), \tag{11}$$

where φ is given as the positive root of (2) and $f(\xi,\zeta_0)$ is given by (Yamamoto, 1959)

$$f=\int_1^\xi\frac{\varphi}{\xi}d\xi. \tag{12}$$

The boundary conditions to be satisfied are as follows:

(i) Diffusion from a ground-level point source of unit strength is to be considered in this paper. In practice a source of small but finite dimensions was set up near the surface. The precise form of this source need not be described here, however, since diffusion very near the source is not explained by means of the diffusivity considered in this study, while the pattern at some distance from the source will not be affected by the detailed form of the source provided that the dimensions of the source are small. The dimensions of the smoke cloud at $x=0$ were taken to be $10z_0$ and $10\alpha^{\frac{1}{2}}z_0$ along z and y directions, respectively.

(ii) Perfect reflection of smoke at the surface was assumed, i.e.,

$$\left(\frac{\partial\chi}{\partial\xi}\right)_{\xi=1}=0. \tag{13}$$

The height $\xi=1$ is regarded as the surface.

In order to solve (11) numerically, it was changed to a finite difference equation,

$$\chi(\Delta)=\chi(0)+\frac{k^2\Delta}{f(\xi)}\frac{1}{h_1^2}\left[\frac{\xi+h_1/2}{\varphi(\xi+h_1/2)}\{\chi(h_1)-\chi(0)\}\right.$$
$$\left.-\frac{\xi-h_1/2}{\varphi(\xi-h_1/2)}\{\chi(0)-\chi(-h_1)\}\right]$$
$$+\frac{k^2\Delta}{f(\xi)}\frac{\xi}{h_2^2}[\chi(h_2)+\chi(-h_2)-2\chi(0)], \tag{14}$$

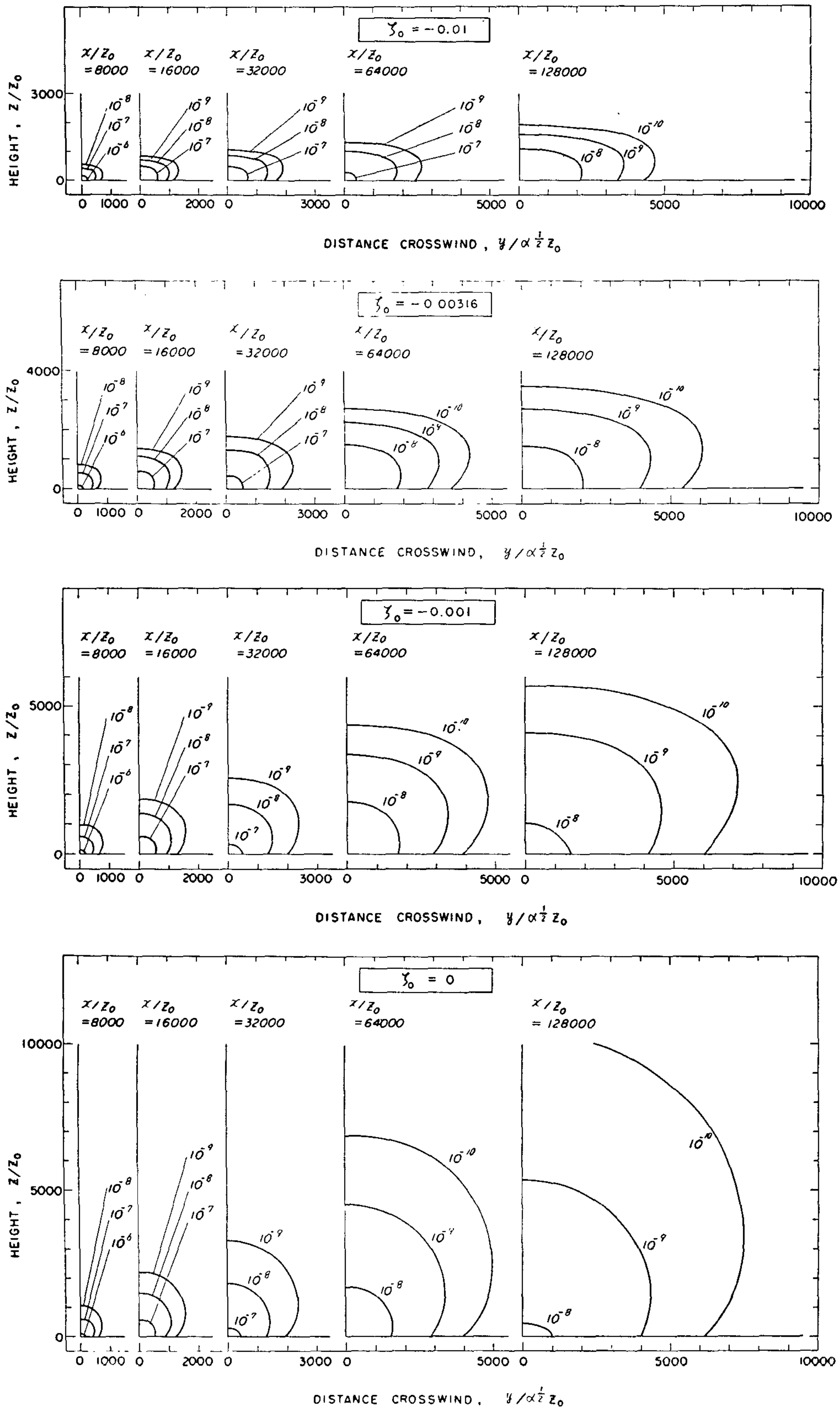

FIG. 1. Isopleths of smoke concentration in several vertical planes across the wind for various stability conditions.

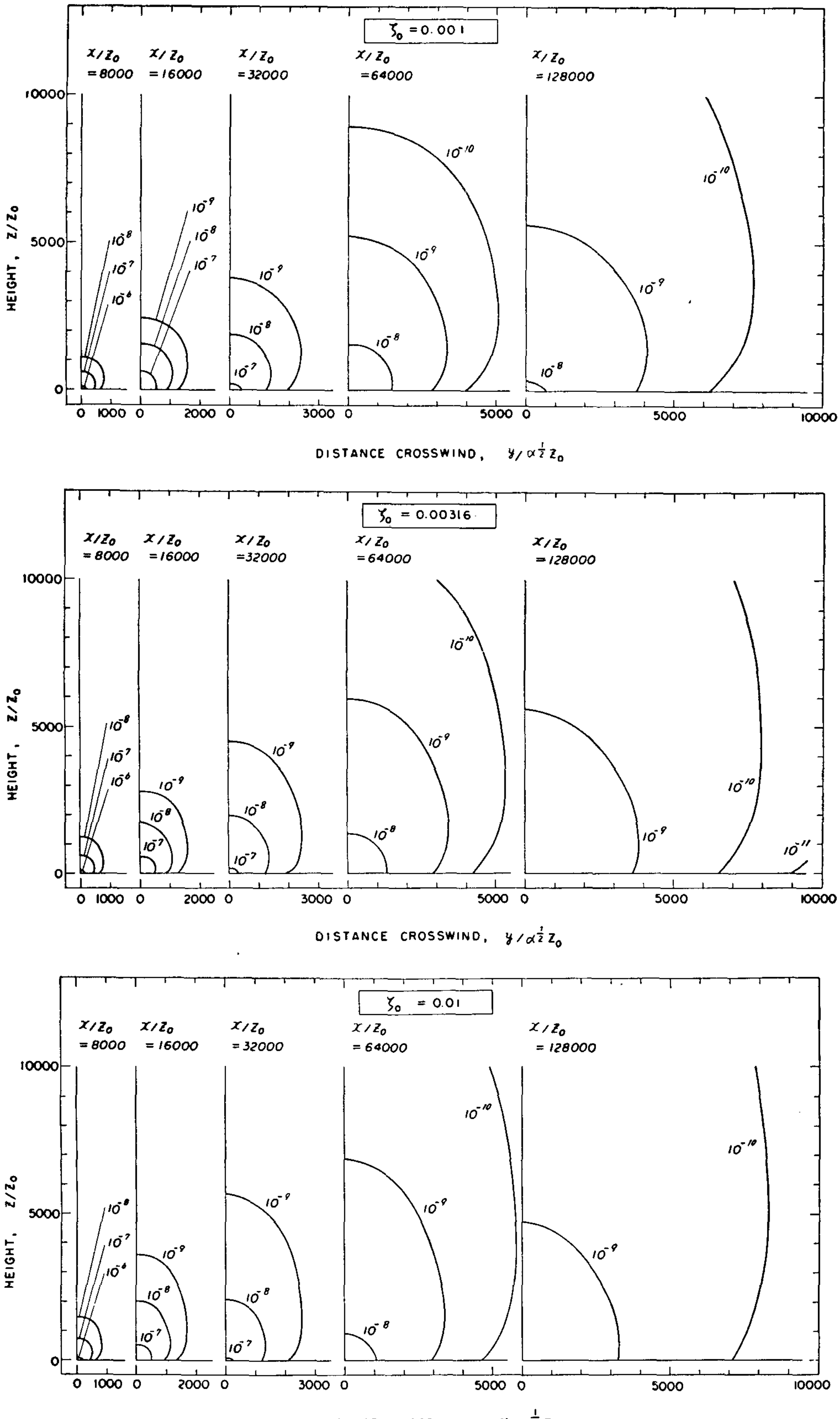

FIG. 1. *Continued.*

with the notations:

$$\chi(\Delta)=\chi\left(\frac{x}{z_0}+\Delta,\frac{y}{\alpha^{\frac{1}{2}}z_0},\ \xi\right),$$

$$\chi(\pm h_1)=\chi\left(\frac{x}{z_0},\frac{y}{\alpha^{\frac{1}{2}}z_0},\ \xi\pm h_1\right),$$

$$\chi(\pm h_2)=\chi\left(\frac{x}{z_0},\frac{y}{\alpha^{\frac{1}{2}}z_0}\pm h_2,\ \xi\right),$$

h_1 and h_2 are the grid intervals along the z and y directions, respectively, Δ the length of one step in the x direction, and $\chi(x,y,z)$ the concentration at a point (x,y,z). The values of χ at $x=0$ were given by the boundary condition (i), and the values of χ at $x/z_0=\Delta_1$, and $\Delta_1+\Delta_2$, $\Delta_1+\Delta_2+\Delta_3$, $\cdots$ were calculated by (14), step by step. The Δ-values were taken as large as allowed by computational stability, for economy of computational time, and Δ-values at each step were not constant. Since the width and height of smoke clouds increase with the downwind distance x, the grid intervals h_1 and h_2 were also changed with the increase in x, and the grid numbers were limited within 30×30.

By integrating (11) with $y/\alpha^{\frac{1}{2}}z_0$ and ξ, and referring to the boundary condition (ii), we obtain the result

$$\int_1^{\infty}d\xi\int_{-\infty}^{+\infty}d\left(\frac{y}{\alpha^{\frac{1}{2}}z_0}\right)f(\xi)\chi\left(\frac{x}{z_0},\frac{y}{\alpha^{\frac{1}{2}}z_0},\ \xi\right)=\text{const}=Q. \quad (15)$$

The constant Q should agree with the source strength, which in our calculation was taken to be unity. The computation of Q was carried out for several values of x and ζ_0 as a check and the extreme value of Q in this calculation was 1.17. This will give a measure of the order of accuracy of the present calculation.

4. Results and discussions

The difference equation (14) was solved numerically (on a IBM 7090) for the following values of ζ_0: 0 (neutral condition), ±0.001 (nearly neutral conditions), ±0.00316 (moderately unstable and stable conditions, respectively), and ±0.01 (very unstable and stable conditions, respectively). The isopleths of the smoke concentration in several vertical planes across the wind are shown in Fig. 1, for each of the above ζ_0 values. In Fig. 1 the ordinate expresses the height in z/z_0 and the abscissa the lateral distance in $y/\alpha^{\frac{1}{2}}z_0$ from the x axis, so that only the vertical spread of smoke is shown directly. The lateral spread of smoke, and particularly its relation with ζ_0, are not yet clear in Fig. 1 because of the unknown parameter α involved in the abscissa.

Fig. 2 shows the configurations of one-tenth of peak concentration found at the center line of the smoke cloud on the ground surface, for different values of ζ_0. The upper part of the figure gives those in the vertical plane through the center line, and the lower part of the figure gives those on the surface. In the vertical plane the position of the one-tenth of peak concentration becomes higher in unstable conditions and lower in stable conditions, with an increase of $|\zeta_0|$. Again the relation between the lateral spread and ζ_0 remains indeterminate.

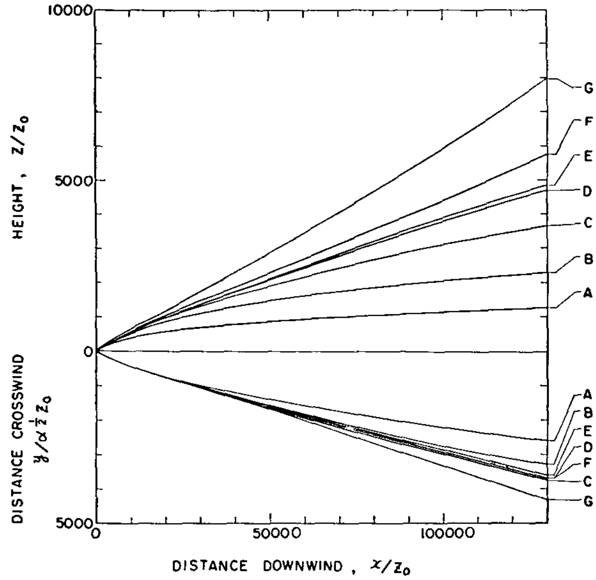

FIG. 2. Profiles of the vertical and lateral spread of smoke, defined by one-tenth of peak concentration. Curves A correspond to $\zeta_0=-0.01$, B to $\zeta_0=-0.00316$, C to $\zeta_0=-0.001$, D to $\zeta_0=0$, E to $\zeta_0=+0.001$, F to $\zeta_0=+0.00316$ and G to $\zeta_0=+0.01$.

We shall now try to evaluate the unknown parameter by comparison of the calculated and the observed results. The observational data used in this study are those obtained during the summer of 1956 at O'Neill, Nebr., under "Project Prairie Grass" (Barad, 1958), and also those obtained during the summer of 1959 at Richland, Wash., under "The Green Glow Diffusion Program" (Barad and Fuquay, 1962). In the latter experiment a fluorescent pigment was used as a tracer, so that the assumption (ii) of perfect reflection by the ground is, strictly speaking, incorrect for this case. The attachment of the particles to the ground and vegetation will diminish the absolute concentration to some extent. However, the cloud width may not change much by this attachment. Despite these expected changes, because so few data are available at present, the use of the Green Glow data is profitable in estimating the dependence of α on the averaging time T and also the effect of z_0 on the diffusion pattern. The roughness parameter z_0 was estimated to be 0.65 cm ($\frac{5}{8}$ cm is used for convenience) at O'Neill, and 20 cm at Richland. The values of ζ_0 were estimated from the measurements of profiles of wind velocity and temperature in individual observations.

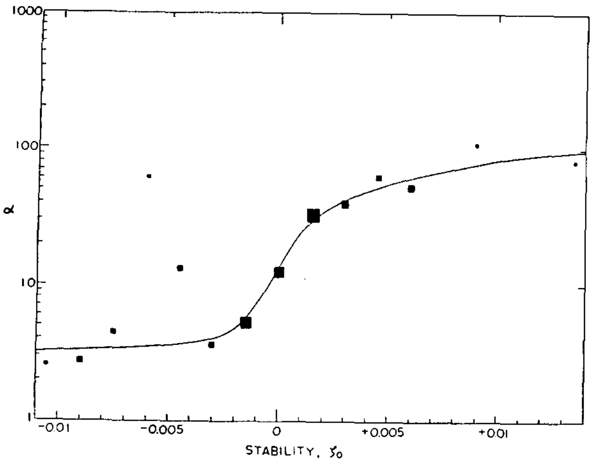

FIG. 3. Values of α evaluated from the Project Prairie Grass data as a function of ζ_0, and a smoothed curve. The area of each square mark is proportional to the number of data.

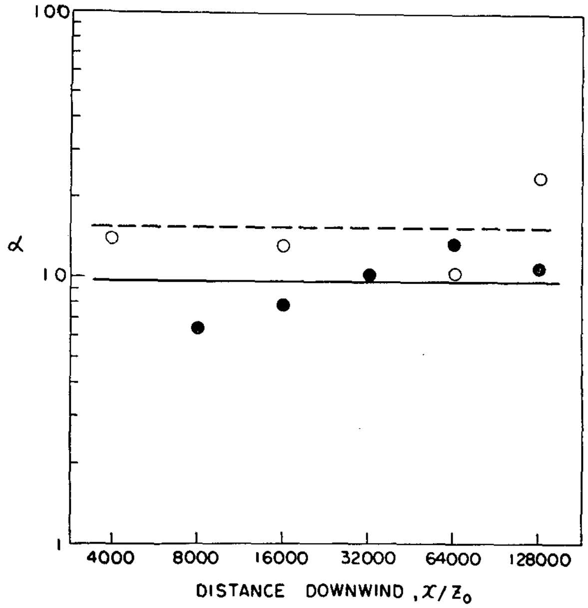

FIG. 4. Values of α, averaged over the observed data in stable conditions, as a function of the distance downwind. Those evaluated from the Prairie Grass data are shown by the black circle and from the Green Glow data by the white circle. Full and broken lines indicate the mean values for the black and white circles respectively.

In order to evaluate α, the lateral spread of smoke at $x/z_0=32{,}000$ and $z/z_0=240$, derived theoretically from Fig. 1, was compared with the lateral distribution observed at $x=200$ m and $z=1.5$ m in Project Prairie Grass, since $z_0=\frac{5}{8}$ cm. From the ratio of the standard deviations of these lateral distributions, the values of $\alpha^{\frac{1}{2}}z_0$ were found, and accordingly the values of α were evaluated for different ζ_0 values. Observational data were classified by taking the interval of ζ_0 to be 0.0015, and the standard deviation was evaluated for the mean distribution. The results are shown in Fig. 3, in which α is taken as ordinate and ζ_0 as abscissa and evaluated values of α are shown by black squares whose areas are taken to be proportional to the numbers of observations in each class. The solid line in the figure represents the presumed mean α-curve. The function $\alpha(\zeta_0,T)$ is found to be monotonically increasing with respect to the stability parameter ζ_0, the value being about 13 in neutral conditions ($\zeta_0=0$), about 3 for $\zeta_0=-0.01$, and about 100 for $\zeta_0=+0.014$.

Recently Fuquay *et al.* (1963) have evaluated the values of the standard deviation of the cross-wind mass distribution, σ_y (meters), from the Green Glow data and the new "30 series" data (comprised of 6 runs in unstable conditions and 9 runs in stable conditions, and obtained on the same grid points as those of the Green Glow to distances of 3200 m downwind). They emphasized rather large fluctuations of σ_y occurring in both stable and unstable conditions and were led to point out the apparent lack of correlation between the width of the plume and thermal stability. It is true that the σ_y- or α-values for individual runs scatter considerably not only for the Green Glow data but also for the Prairie Grass data. However, in connection with the present analysis of the dependence of α on stability, we are rather interested in the small, but clear differences of the σ_y values between mean Green Glow and mean "30 series" (see Fig. 2 of their paper). Because the "30 series" includes 9 runs of stable cases together with 6 runs of unstable cases, it is obvious that the effect of stability on σ_y is diluted in their comparison. Further, it should be noted that the observed σ_y values are nearly proportional to $\alpha^{\frac{1}{2}}$, so that the variation of σ_y with stability is far less than that of α with stability. Therefore we consider that the results shown in Fig. 2 of their paper are not necessarily in contradiction to the results of the present analysis. The "30 series" data should be analysed so as to determine the relation between α or σ_y and stability in detail.

Next the dependence of α on the averaging time T was examined by comparing the evaluated values of α from the Prairie Grass data ($T=10$ minutes) and from the Green Glow data ($T=30$ minutes). In this case to make the comparison reasonable, the data in stable conditions were used, because the Green Glow data cover only the stable conditions. In addition, instead of classifying the data by the values of ζ_0, the lateral distribution of smoke was averaged over the data in every stable condition observed. The values of α were evaluated for different values of x/z_0, as shown in Fig. 4, in which those evaluated from the Prairie Grass data are indicated by the solid circles and those from the Green Glow data by the white circles. The solid and broken lines in the figure indicate the presumed mean values of α for Prairie Grass and Green Glow, respectively. Fig. 4 indicates that the ratio of α for $T=30$ minutes to that for $T=10$ minutes is about 1.6, or that

α is approximately proportional to $T^{0.43}$. The values of α given by the curve in Fig. 3 are, therefore, applicable only for $T=10$ minutes, and for other values of T the change of α with T, shown above, should be taken into account. However, in order to establish the α-T relation definitely, more data for different values of T covering both stable and unstable conditions are needed.

The evaluation of $\alpha(\zeta_0,T)$ has thus far been based only on surface observations. In order to examine the validity of (9) at high levels, the observed concentration, χ_{obs}, was reduced to the non-dimensional form χ used in the present work. The observed concentration, χ_{obs}, derived from a point source of strength Q' must satisfy the following condition of continuity

$$\int_{z_0}^{\infty} dz \int_{-\infty}^{\infty} dy u\chi_{\text{obs}} = Q'. \tag{16}$$

The non-dimensional concentration χ from a point source of unit strength also is required to satisfy (15) with $Q=1$. From (15) and (16) with $Q=1$, the relation between χ and χ_{obs} is given by

$$\chi = \frac{\alpha^{\frac{1}{2}} z_0^2 u_*}{kQ'} \chi_{\text{obs}}. \tag{17}$$

After the values of χ_{obs} were reduced to non-dimensional form by (17), they were divided by the theoretical peak concentrations of the respective stability conditions. Similarly the observed lateral distances from the center axis of the smoke pattern were divided by $\alpha^{\frac{1}{2}}z_0$ so as to reduce them to the non-dimensional distances, and were again divided by the lateral standard deviations of the corresponding theoretical patterns. In the processes of these reductions the values of α obtained from the curve in Fig. 3 were used for the Prairie Grass data ($T=10$ minutes), and 1.6 times them were used for the Green Glow data ($T=30$ minutes). Thus it is expected that the reduced lateral distributions of smoke concentration at a given height will agree with the reduced theoretical profile with unit peak concentration and unit standard deviation, if the assumed equation (9) is correct. The test was made on the lateral distributions at $x/z_0=16{,}000$, and at $\xi=47.5$ ($z=9.5$ m) and $\xi=281$ ($z=56.2$ m) for the Green Glow data, and at $\xi=400$ ($z=2.5$ m), $\xi=720$ ($z=4.5$ m), and $\xi=1200$ ($z=7.5$ m) for the Prairie Grass data, as shown in Fig. 5. The expected theoretical profile is shown by the solid curve in the figure and the observed profiles in unstable, near neutral and stable conditions are shown by the cross mark, solid circle, and white circle, respectively. It is seen in Fig. 5 that no systematic differences exist among the unstable, near neutral and stable conditions.

In the Green Glow cases the scattering of the observed concentrations is considerable and some asymmetry is observed. However, the observed distributions are not far from the theoretical one in general. In the Prairie Grass data at $\xi=400$ ($z=2.5$ m) agreement of the observed and theoretical profiles is remarkably good. On the other hand at $\xi=720$ ($z=4.5$ m) the observed peak concentrations at this height exceed the theoretical one and at $\xi=1200$ ($z=7.5$ m) this tendency becomes more pronounced. This result of the analysis of the Prairie Grass data means that at high levels the vertical spread of smoke is more pronounced than that predicted by the present theory. However, because of the empirical nature of the present method we cannot say whether this discrepancy is due to incorrectness of the assumption for K_y in (9) or of the assumption for K_z in (1). For the Prairie Grass data, it will be noticed that at $\xi=720$, and $x/z_0=16{,}000$, where the observed profiles begin to deviate from the theoretical one, the smoke concentrations are about one-tenth of the surface peak concentration (see Fig. 2), and at $\xi=1200$ ($z=7.5$ m) they are about 1.5 per cent of the surface peak concentration in neutral conditions. Therefore within the range of one-tenth of peak concentration, which is considered to be the height of the smoke, the observed profiles agree fairly well with the theoretical ones. It may be concluded therefore that the assumed form of (9) for K_y, together with that of (1) for K_z, holds at least in this range. It will also be noticed in Fig. 5 that the Gaussian distribution for the observed lateral profiles is a good approximation at every level.

The unknown parameter α is now determined as a function of ζ_0 and T, and we can obtain detailed diffusion patterns from Fig. 1 and crude ones from Fig. 2. For instance, if the values of α given in Fig. 3 are inserted in Fig. 1 or 2, one can obtain the diffusion patterns for $T=10$ minutes, which retain the general features of the observed ground-level point source diffusion patterns. It can be seen that the ratio of the lateral spread of smoke to the vertical one is greater than unity in any stability condition, and that the ratio is greater in unstable conditions than in stable conditions. The former result is an obvious one, but the latter seems somewhat puzzling; it would be natural to imagine that buoyancy forces make the vertical mixing (or diffusion) more pronounced compared to lateral mixing in unstable conditions than in stable conditions. A possibility of explaining this puzzling result may be sought for in the restriction of the vertical turbulent motion by the existence of the ground surface. In an unstable condition, buoyancy forces may cause an increase of vertical mixing within this restriction. At the same time, because of the complex motions of the eddies, some lateral turbulent (or internal) forces may be induced, which should be zero averaged over all eddies, but which may cause a larger increase in lateral mixing, because of less restriction of motion in this direction. A support for this consideration may be found in Table 1, in which the values of the non-dimensional diffusivities, K_y/kz_0u_* and K_z/kz_0u_*, and their ratio,

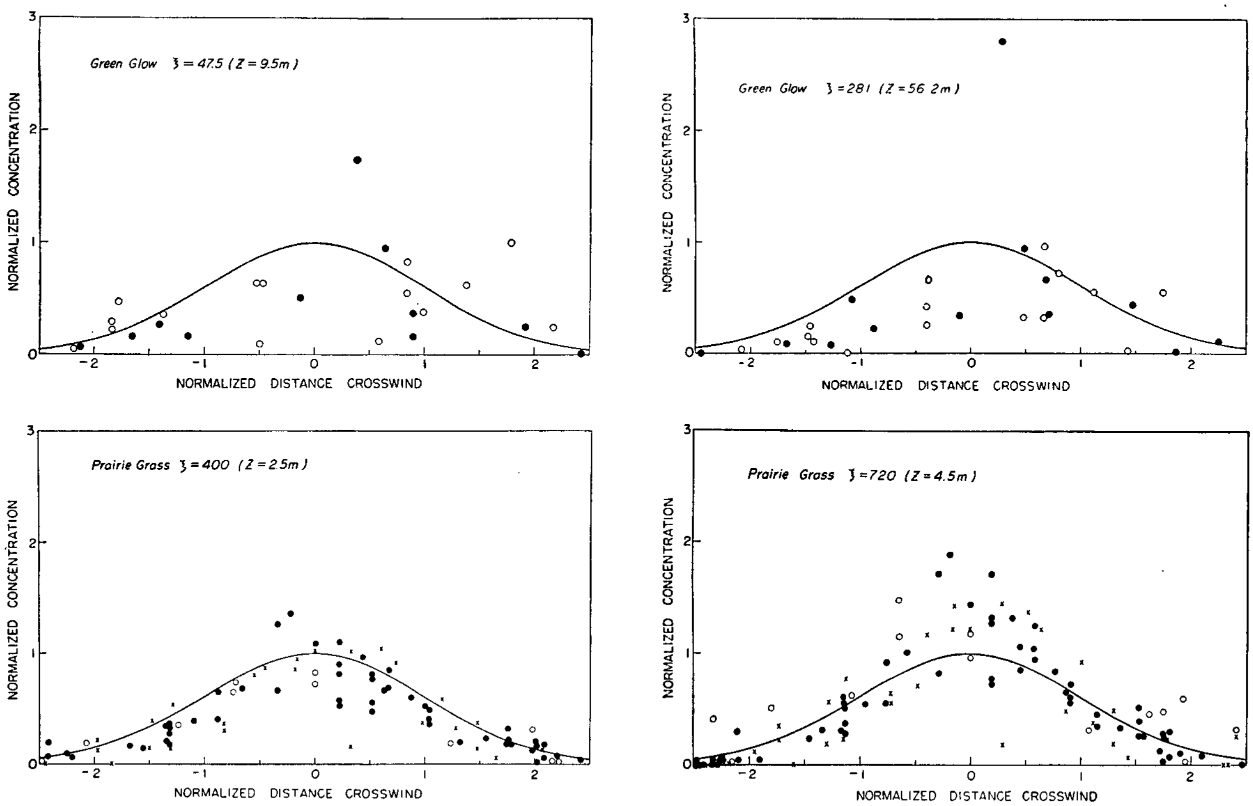

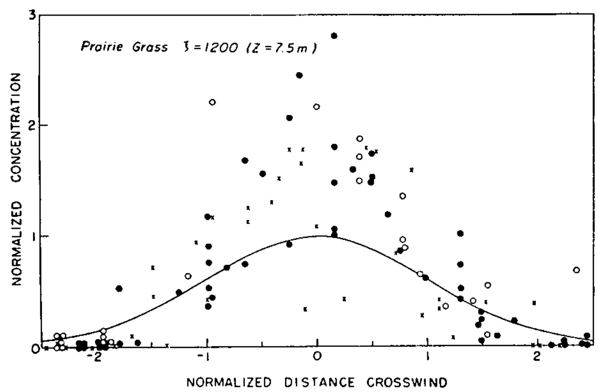

FIG. 5. Values of the normalized concentration against the normalized distance cross-wind at $x/z_0=16{,}000$. Observed values in stable conditions are shown by the white circle, those in near neutral conditions by the black circle, and those in unstable conditions by the cross mark. The curve indicates the theoretical distribution.

TABLE 1. Values of K_y/kz_0u_*, K_z/kz_0u_*, and K_y/K_z as functions of ξ and ζ_0.

		ζ_0 -0.01	-0.001	0	0.001	0.01
$\xi=100$	K_y/kz_0u_*	320	730	1300	2500	8500
	K_z/kz_0u_*	72	97	100	102	122
	K_y/K_z	4.4	7.5	13	25	70
$\xi=1000$	K_y/kz_0u_*	3200	7300	13,000	25,000	85,000
	K_z/kz_0u_*	100	720	1000	1220	2200
	K_y/K_z	32	10	13	20	39
$\xi=10{,}000$	K_y/kz_0u_*	32,000	73,000	130,000	250,000	850,000
	K_z/kz_0u_*	100	1000	10,000	22,000	45,000
	K_y/K_z	320	73	13	11	19

K_y/K_z, are tabulated for several values of ξ and ζ_0. Table 1 shows that both K_y/kz_0u_* and K_z/kz_0u_* increase with height regardless of the stability conditions. It shows, however, that the ratio K_y/K_z increases with height in stable conditions, while it decreases with height in unstable conditions. As a consequence, the puzzling result mentioned above, which corresponds to the increase of K_y/K_z from stable to unstable conditions in Table 1, occurs only in the lowest layer ($\xi=100$), and it disappears in the middle layer ($\xi=1000$), and the reverse tendency, that K_y/K_z is greater in stable conditions than in unstable conditions, appears in the highest layer ($\xi=10{,}000$), where the restriction of vertical motion by the surface will be negligible.

Next examine the calculated diffusion patterns in more detail. Fig. 6 shows the relation between the peak concentration at the surface and the distance downwind for different values of ζ_0. It was shown by Sutton (1953) that the empirical relation based on observations in near

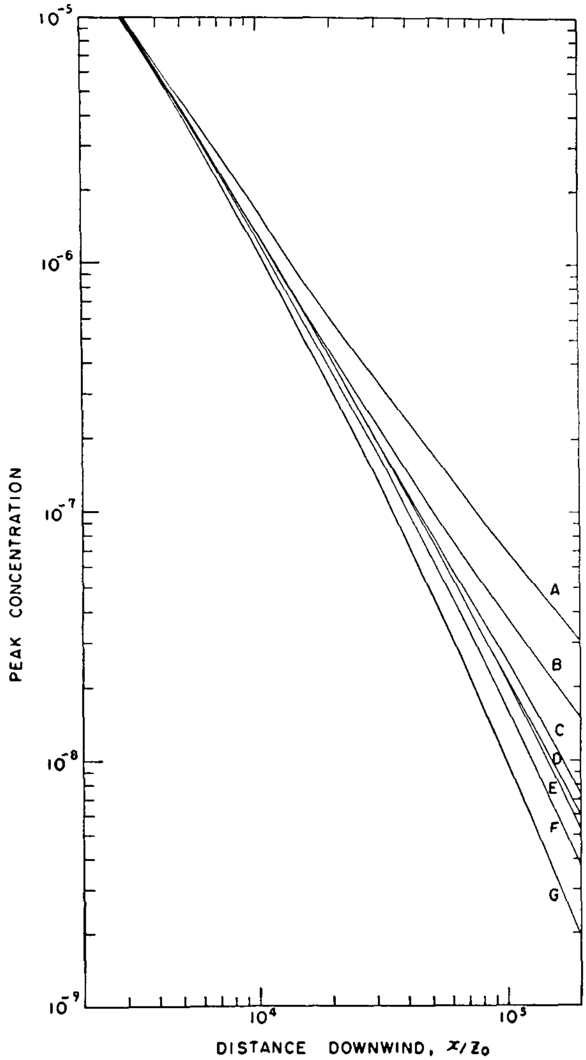

FIG. 6. Curves of the surface peak concentration against the distance downwind. The curve A corresponds to $\zeta_0 = -0.01$, B to $\zeta_0 = -0.00316$, C to $\zeta_0 = -0.001$, D to $\zeta_0 = 0$, E to $\zeta_0 = +0.001$, F to $\zeta_0 = +0.00316$ and G to $\zeta_0 = +0.01$.

neutral conditions is given by a power law,

$$\chi(x,0,z_0) \propto x^{-p}, \tag{18}$$

with $p = 1.76$. The calculated result in neutral conditions shown in Fig. 6 is expressed by

$$\chi(x/z_0,0,1) \propto (x/z_0)^{-1.78}, \tag{19}$$

in the middle range of x/z_0. This agrees with the observed result. Fig. 6 further shows that in both unstable and stable conditions the calculated results deviate from a straight line on a log-log scale, or deviate from a power law relation with increases in the diabaticity and distance downwind.

It will therefore be necessary to compare the calculated results in diabatic conditions with the observed ones. In this context it would not be appropriate to plot the observed results in Fig. 6, because while there are so many data to be considered, the calculated deviations of the diabatic cases from the neutral one are not large as seen in Fig. 6, and complication of the resulting figure would be inevitable. To avoid this complication, the observed peak concentrations are given versus the stability parameter ζ_0 in Fig. 7, for three different distances downwind, i.e., $x/z_0 = 8000$, 16,000 and 128,000. It is noted that at both O'Neill and Richland the surface observations were made at 1.5 m above the surface, which corresponds to $\xi = 240$ at O'Neill and to $\xi = 7.5$ at Richland. Therefore the calculated peak concentrations at these values of ξ are shown in the figure; the solid line corresponds to $\xi = 7.5$ and the broken line to $\xi = 240$. It will be seen from these figures that agreement between observed and calculated peak concentrations is fairly good for Prairie Grass when the distance downwind is not very large. Recalling the scarcity of data for Green Glow and the expected depletion of concentration by absorption or attachment of smoke on the ground surface, one may note that the calculated peak concentrations generally agree with observations in diabatic conditions also.

5. Conclusions

The lateral diffusivity near the ground is formulated in equation (9). Values of α are given in Fig. 3, for the case of $T = 10$ minutes. It was shown that α increases as $T^{0.43}$, although this relation needs to be checked by further observations. The present analysis allows the diffusion patterns in different stability and surface conditions to be predicted fairly well, by means of the charts given in Fig. 1, together with the values of α in Fig. 3 and the necessary corrections to them for different values of T.

Acknowledgment. The authors express their thanks to Mr. C. Bristor and his group at the United States Weather Bureau for handling of the computations on the computer.

REFERENCES

Barad, M. L., 1958: Project Prairie Grass, A field program in diffusion. *Geophysical Research Papers*, No. 59, Vols. 1, and 2, AFCRC-TR-58-235, Geophysics Research Directorate, Air Force Cambridge Research Center, Bedford, Mass., 280 pp. and 209 pp.

——, and J. J. Fuquay, 1962: The Green Glow diffusion program. *Geophysical Research Papers*, No. 73, Vols. 1 and 2, AFCRL-62-251, Geophysics Research Directorate, Air Force Cambridge Research Laboratories, Bedford, Mass., 77 pp. and 305 pp.

Deacon, E. L., 1949: Vertical diffusion in the lowest layers of the atmosphere. *Quart. J. R. meteor. Soc.*, **75**, 89–103.

Ellison, T. H., 1957: Turbulent transport of heat and momentum from an infinite rough plane. *J. fluid Mech.*, **2**, 456–466.

Fuquay, J. J., C. L. Simpson, M. L. Barad and J. H. Taylor, 1963: Results of recent field programs in atmospheric diffusion. *J. appl. Meteor.*, **2**, 122–128.

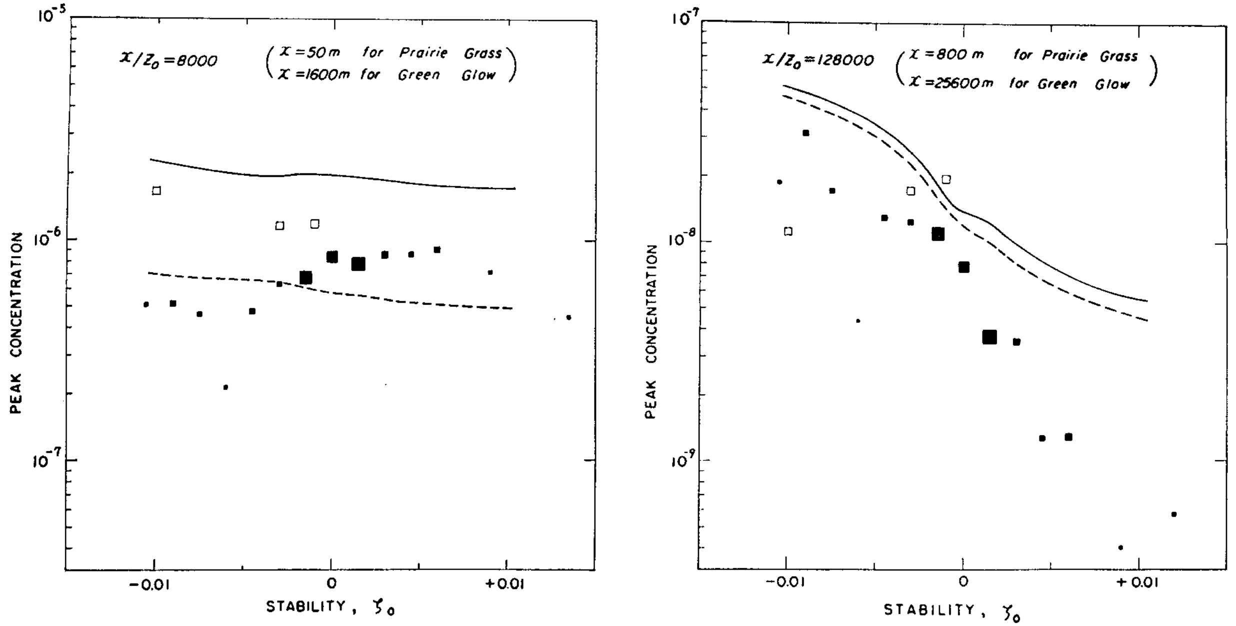

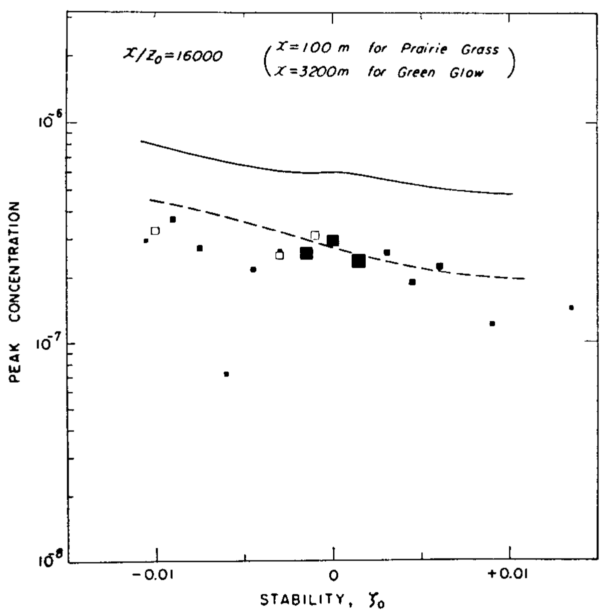

FIG. 7. Values of peak concentration at 1.5 m height (i.e., $\xi=240$ for the Prairie Grass data and $\xi=7.5$ for the Green Glow data). Those evaluated from the Prairie Grass data are shown by the black square, and those from the Green Glow data by the white square. The area of the squares is proportional to the number of data. The full line indicates the theoretically expected values for Green Glow and the broken line for Prairie Grass.

Kondo, J., 1962: Observations on wind and temperature profiles near the ground. *Sci. Rep. Tohoku Univ., Ser.* 5, 14, 41–56.

Monin, A. S., and A. M. Obukhov, 1954: Basic regularity in turbulent mixing in the surface layer of the atmosphere. *Akademia Nauk. SSSR Geofiz. Inst. Trudy*, 151, 163–187.

Panofsky, H. A., A. K. Blackadar and G. E. McVehil, 1960: The diabatic wind profile. *Quart. J. R. meteor. Soc.*, 86, 390–398.

Shimanuki, A., 1961: Diffusion from the continuous source with finite release time. *Sci. Rep. Tohoku Univ. Ser.* 5, 12, 184–190.

Sutton, O. G., 1953: *Micrometeorology*. New York, McGraw-Hill, 333 pp.

Yamamoto, G., 1959: Theory of turbulent transfer in non-neutral conditions. *J. meteor. Soc. Japan, Ser.* 2, 37, 60–70.

——, and A. Shimanuki, 1960: Numerical solution of the equation of atmospheric turbulent diffusion. *Sci. Rep. Tohoku Univ. Ser.* 5, 12, 24–35.